Neuron, Vol. 38, 611–624, May 22, 2003, Copyright ©2003 by Cell Press

Activation of PI3-Kinase Is Required for AMPA Receptor Insertion during LTP of mEPSCs in Cultured Hippocampal Neurons

Heng-Ye Man,[2] Qinhua Wang,[2] Wei-Yang Lu,[3] William Ju,[2] Gholamreza Ahmadian,[2] Lidong Liu,[1,2] Sandra D'Souza,[2] T.P. Wong,[1,2] C. Taghibiglou,[1,2] Jie Lu,[1,2] Larry E. Becker,[2] Lin Pei,[4] Fang Liu,[4] Matthias P. Wymann,[6] John F. MacDonald,[5] and Yu Tian Wang[1,2,*]

[1]Brain Research Centre and Department of Medicine
Vancouver Hospital and Health Science Centre
University of British Columbia
Vancouver, British Columbia V6T 2B5
[2]Brain and Behavior Program and
Department of Pathology
Research Institute of the
Hospital for Sick Children and
Departments of Laboratory Medicine
and Pathobiology
University of Toronto
[3]Department of Anesthesia
University of Toronto and
Trauma Research Program
Sunnybrook and Women's College
Health Sciences Centre
[4]Department of Psychiatry
University of Toronto and
Department of Neuroscience
Centre for Addiction and
Mental Health Clarke Division
[5]Department of Physiology
University of Toronto
Toronto, M5S 1A8
Canada
[6]Institute of Biochemistry
University of Fribourg
CH-1700 Fribourg
Switzerland

Summary

Hippocampal CA1 homosynaptic long-term potentiation (LTP) is expressed specifically at activated synapses. Increased insertion of postsynaptic α-amino-3-hydroxy-5-methyl-isoxazole-4-propionic acid receptors (AMPARs) appears to be crucial for CA1 LTP. However, the mechanism underlying AMPAR insertion during LTP remains largely unknown. We now report that phosphatidylinositol 3-kinase (PI3K) is complexed with AMPARs at synapses and activated by selective stimulation of synaptic N-methyl-D-aspartate (NMDA) receptors. Activation of the AMPAR-associated PI3K is required for the increased cell surface expression of AMPARs and LTP. Thus, our results strongly suggest that the AMPAR-PI3K complex may constitute a critical molecular signal responsible for AMPAR insertion at activated CA1 synapses during LTP, and consequently, this lipid kinase may serve to determine the polarity of NMDA receptor-dependent synaptic plasticity.

*Correspondence: ytwang@interchange.ubc.ca

Introduction

Long-term changes, long-term potentiation (LTP) and depression (LTD), in synaptic efficacy observed at the glutamatergic synapses of the CA1 region of the hippocampus have been considered as candidates for the cellular substrates of learning and memory (Bear and Malenka, 1994; Bliss and Collingridge, 1993; Malenka and Nicoll, 1999; Soderling and Derkach, 2000; Zhuo and Hawkins, 1995). Both LTP and LTD are synapse specific, i.e., they are expressed specifically at activated synapses (Bear and Malenka, 1994; Bliss and Collingridge, 1993; Daw et al., 2002; but also see Nishiyama et al., 2000). However, the mechanisms mediating the synapse specificity remain elusive. It has been proposed that activation of the postsynaptic N-methyl-*D*-aspartate (NMDA) subtype of glutamate receptors is required for both LTP and LTD and that Ca^{2+} influx through the activated NMDA receptors (NMDARs) triggers a series of intracellular cascades that lead to alteration of α-amino-3-hydroxy-5-methyl-isoxazole-4-propionic acid receptor (AMPAR) function and, hence, result in either the potentiation or depression of AMPAR-mediated synaptic transmission (Bear and Malenka, 1994; Bliss and Collingridge, 1993; Malenka and Nicoll, 1999; Soderling and Derkach, 2000; Zhuo and Hawkins, 1995). However, the mechanisms of altering AMPAR-mediated transmission during LTP and LTD remain hotly debated. Evidence accumulated recently seems to strongly suggest that activity-dependent changes in functional postsynaptic AMPAR numbers, as a consequence of altered redistribution or a change in their trafficking at the postsynaptic membrane, may represent a unified mechanism underlying the expression of both LTP and LTD (Malenka and Nicoll, 1999; Malinow et al., 2000; Man et al., 2000a; Sheng and Lee, 2001). Indeed, both increased AMPAR insertion and endocytosis at the postsynaptic membrane have been described during LTP (Hayashi et al., 2000; Liao et al., 2001; Lu et al., 2001) and LTD (Kim et al., 2001; Luscher et al., 1999; Man et al., 2000b; Wang and Linden, 2000), respectively. However, it remains unclear how activation of NMDARs can be translated into enhanced AMPAR insertion during LTP or endocytosis during LTD. In the present work, we provide evidence to suggest that the class IA phosphatidylinositol 3-kinase p85α/p110α (PI3K), a lipid kinase that phosphorylates phosphoinositides [PtdIns (4,5) P_2] at the 3′ position of the inositol ring and generates PtdIns (3,4,5) P_3 (PtdIns-3P) (De Camilli et al., 1996; Vanhaesebroeck et al., 1997; Wymann and Pirola, 1998), may play an important role in mediating the selective insertion of AMPARs at activated synapses during the expression of LTP.

Results

To investigate the potential role of PI3K in mediating AMPAR trafficking during LTP and/or LTD, we utilized

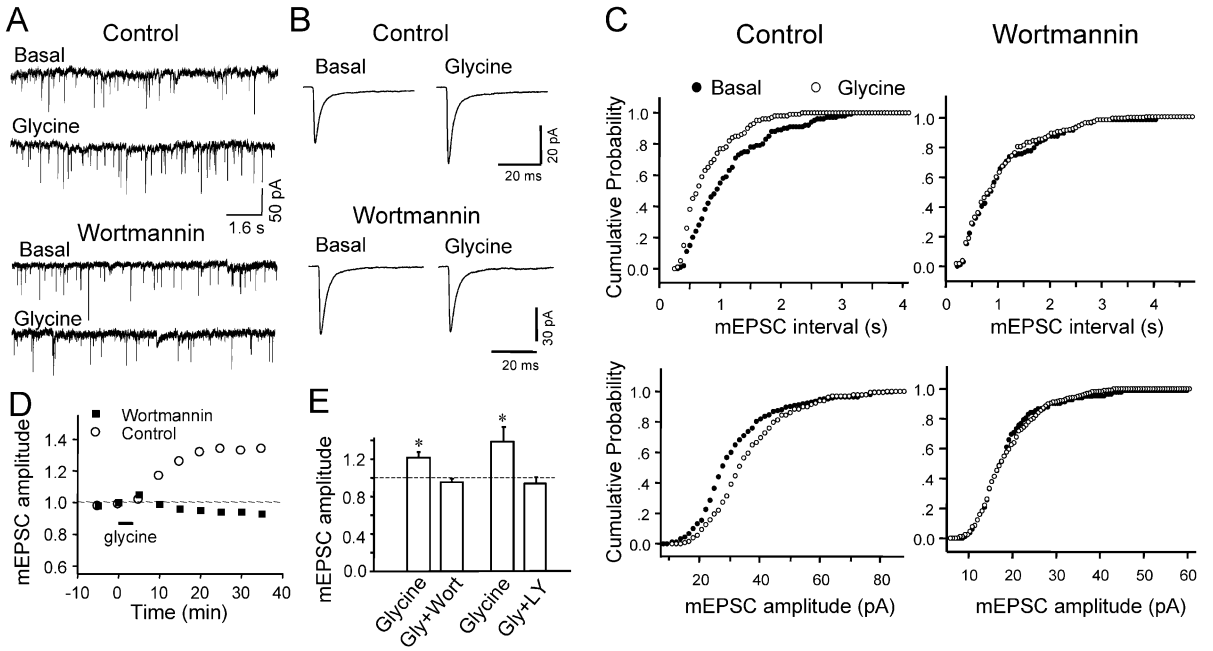

Figure 1. PI3K Is Required for Glycine-Induced LTP of mEPSCs in Cultured Hippocampal Neurons

Cultured hippocampal neurons were either incubated in extracellular solution (ECS; control) or ECS supplemented with wortmannin (100 nM; Wortmannin) 10 min before and throughout the recording period. (A) Examples of continuous recordings from individual neurons immediately before (Basal) and 20 min after glycine application (Glycine, 200 μM). (B) Examples of individual mEPSCs averaged from 120 events before (Basal) and 20 min after glycine (Glycine). (C) Cumulative probability plots for mEPSC amplitudes and interevent intervals obtained before (Basal) and 20 min after glycine (Glycine, 200 μM; 3 min). mEPSC amplitudes are normalized to the values from the initial 5 min and plotted over time in (D). In the absence of the PI3K inhibitor wortmannin (Control), brief application of glycine in the bath solution reliably induces LTP of $mEPSC_{AMPA}$, as reported previously (Lu et al., 2001). Treatment of neurons with wortmannin (Wortmannin; 100 nM) has no effect on basal mEPSCs over the time course of recordings, but in the presence of wortmannin, glycine was no longer capable of producing LTP. (E) Amplitude histogram summarizes data from groups of individual neurons treated with glycine (200 μM; 5 min) in the absence or presence of PI3K inhibitors wortmannin (100 nM) or LY294002 (10 μM). Responses obtained 20 min after glycine treatment were normalized to the values from the initial 5 min of recording. Glycine produced LTP which is prevented by inhibition of PI3K with wortmannin (1.23 ± 0.05, n = 6 for glycine versus 0.96 ± 0.03, n = 4 for Gly + Wort) or with LY294002 (1.41 ± 0.16, n = 10 versus 0.96 ± 0.06, n = 6). *$p < 0.05$.

recently developed LTP (Liao et al., 2001; Lu et al., 2001) and LTD (Carroll et al., 1999) models in cultured hippocampal neurons. Miniature excitatory postsynaptic currents (mEPSCs) in cultured hippocampal neurons were recorded under whole-cell configuration. These mEPSCs are comprised of two pharmacologically distinct components: a prominent fast component mediated by AMPARs ($mEPSC_{AMPA}$) and a much smaller and slower component mediated by NMDARs ($mEPSC_{NMDA}$) (Lu et al., 2001). Similar to the electrically evoked EPSCs in CA1 neurons in hippocampal slices (Bear and Malenka, 1994; Bliss and Collingridge, 1993; Zorumski and Thio, 1992), the mEPSCs can exhibit either LTP (Lu et al., 2001) or LTD (Carroll et al., 1999; Lu et al., 2001), depending upon the ways by which NMDARs are pharmacologically activated (Lu et al., 2001). As shown in Figure 1, application of the NMDAR coagonist glycine (200 μM; 3 min) produced LTP of mEPSCs, as shown by the persistent increase in both amplitude and frequency, specifically the $mEPSC_{AMPA}$ component (Lu et al., 2001) (see also Figure 3E; the amplitude and frequency of mEPSCs 20 min after glycine being 1.23 ± 0.06 and 1.34 ± 0.07 of the controls, respectively; n = 6; $p < 0.01$). This particular form of potentiation of mEPSCs shares several similarities with the well-characterized hippocampal CA1 homosynaptic LTP observed in slice preparations: it requires Ca^{2+} influx through activated postsynaptic NMDARs and results from an increase in the plasma membrane insertion of postsynaptic AMPARs (Lu et al., 2001). The increased mEPSC frequency is likely due to the addition of events (following glycine-induced receptor insertion) that were previously below the detection threshold. The glycine-induced LTP of mEPSCs is in striking contrast to the LTD of mEPSCs produced by stimulation of NMDARs with bath application of NMDA (10 μM; 3 min) (Beattie et al., 2000; Lu et al., 2001; Figure 2). This LTD of mEPSCs resembles the CA1 homosynaptic LTD characterized in hippocampal slices (Bear and Malenka, 1994): it requires NMDA channel-gated Ca^{2+} influx, activation of calcineurin, and subsequent stimulation of clathrin-dependent endocytosis of AMPARs (Beattie et al., 2000).

What are the intracellular signaling pathways that produce either net AMPAR insertion or internalization, thereby dictating the expression of these two opposing forms of NMDAR-dependent synaptic plasticity? Among many potential intracellular factors involved in mediating plasma membrane protein trafficking, we investigated the potential role of PI3K. Activation of this lipid kinase has recently been implicated in both plasma membrane protein insertion (De Camilli et al., 1996; Passafaro et al., 2001; Pessin et al., 1999) and internalization processes

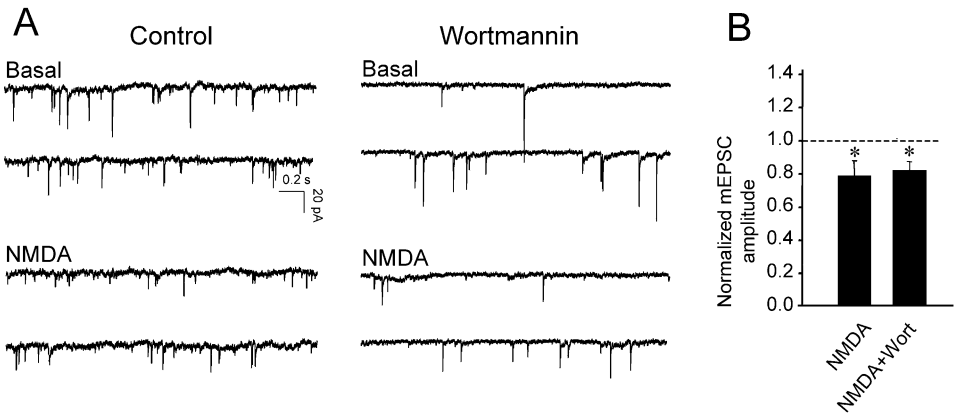

Figure 2. PI3K Is Not Involved in NMDA-Induced LTD of mEPSCs in Cultured Hippocampal Neurons

(A) Examples of continuous recordings immediately before (Basal) and 20 min after NMDA application (NMDA, 20 μM plus 10 μM glycine; 5 min) from individual neurons incubated with ECS (Control) or ECS supplemented with 100 nM wortmannin (Wortmannin) 10 min prior to NMDA application and throughout the recording period.

(B) Amplitude histogram summarizes data from groups of individual neurons treated with NMDA (20 μM plus 10 μM glycine) in the absence (NMDA; n = 6) or the presence of 100 nM wortmannin (NMDA + Wort; n = 4). Responses obtained 20 min after glycine treatment were normalized to the values from the initial 5 min of recording. Inhibition of PI3K has little effect on NMDA-induced LTD (0.78 ± 0.08 for NMDA versus 0.81 ± 0.08 for NMDA + Wort).

(Rapoport et al., 1997; Shpetner et al., 1996). To determine whether PI3K plays any role in mediating either LTP or LTD of mEPSCs, wortmannin (100 nM), a PI3K inhibitor (Wymann et al., 1996), was bath applied to cultured hippocampal neurons 10 min prior to bath application of either glycine or NMDA and was present throughout the recording period. Wortmannin produced little effect on the basal mEPSCs (amplitude and frequency before and 20 min after wortmannin being 24.48 ± 1.73 pA versus 22.1 ± 1.02 pA and 2.32 ± 0.37/s versus 2.09 ± 0.25/s; n = 7; $p > 0.05$). However, as shown in Figure 1, wortmannin abolished the ability of glycine to induce LTP of mEPSCs. The amplitude of mEPSCs after glycine application was 1.23 ± 0.05 (n = 6) and 0.96 ± 0.03 (n = 6) -fold of the controls in the absence and the presence of wortmannin, respectively (Figures 1A–1E). Moreover, a similar blockade was obtained when LY294002 (10 μM), another, more specific, inhibitor of PI3K (Kuruvilla et al., 2000), was employed (Figure 1E). In dramatic contrast, as shown in Figure 2, we found that PI3K inhibition had little effect on the NMDA-induced LTD of mEPSCs: the amplitudes of mEPSCs after NMDA application were 0.78 ± 0.08 (n = 5) and 0.80 ± 0.03 (n = 4), respectively. Thus, PI3K is specifically required for glycine-induced LTP but not NMDA-induced LTD.

We next determined whether exogenous PI3K application was sufficient to produce a lasting potentiation of mEPSCs (Figure 3) by using an active or a heat-inactivated recombinant PI3K complex of p85α/p110α (Figure 3C) applied intracellularly through the recording pipette. As shown in Figures 3A, 3B, and 3D, within a few minutes of the start of whole-cell recording, intracellular perfusion of active but not heat-inactivated PI3K resulted in an increase in both the amplitude and frequency of mEPSCs. The potentiation of mEPSCs typically peaked within 10 min, and was maintained thereafter for the entire recording period. The normalized amplitude and frequency following 30 min of recording were 1.25 ± 0.05 and 1.35 ± 0.07 with active PI3K (n = 6) and 1.01 ± 0.03 and 0.99 ± 0.04 for cells recorded with heat-inactivated PI3K (n = 4; Figure 3D), respectively. Moreover, once the potentiation of mEPSCs by PI3K was established, glycine was no longer capable of inducing LTP of mEPSCs (Figure 3E). Thus, normalized $mEPSC_{AMPA}$ amplitude and frequency 30 min after glycine application were 0.99 ± 0.05 and 1.02 ± 0.03 for cells (n = 3) perfused with active PI3K compared with 1.23 ± 0.06 and 1.34 ± 0.07 for cells (n = 6) recorded with standard pipette solution (Figure 3E), respectively. Taken together, these results strongly suggest that PI3K activation is both necessary and sufficient for the glycine-dependent LTP of mEPSCs by synaptic NMDARs.

We previously demonstrated that glycine-induced LTP is largely mediated by a rapid increase in the number of postsynaptic AMPARs as a result of facilitated AMPAR insertion (Lu et al., 2001). The necessity and sufficiency of PI3K in glycine-induced LTP is consistent with a requirement for its activity in the glycine-induced increase in plasma membrane insertion of AMPARs. We next investigated this possibility by measuring the cell surface expression of AMPARs using a quantitative cell surface ELISA assay (Lu et al., 2001; Man et al., 2000b). We found that application of glycine produced an increase in the cell surface expression of AMPARs, and this increase was prevented by pretreatment with LY294002 and significantly inhibited by pretreatment with wortmannin (Figure 4A). Since cell surface expression can be modified by either insertion or endocytosis, we examined both of these aspects of AMPAR trafficking, in the presence and absence of PI3K inhibitors, in control and glycine-treated hippocampal cultures. Specific detection of newly inserted AMPARs was performed using our recently developed AMPAR insertion assay (Lu et al., 2001). In this assay, preexisting cell surface AMPARs were first blocked by incubation of

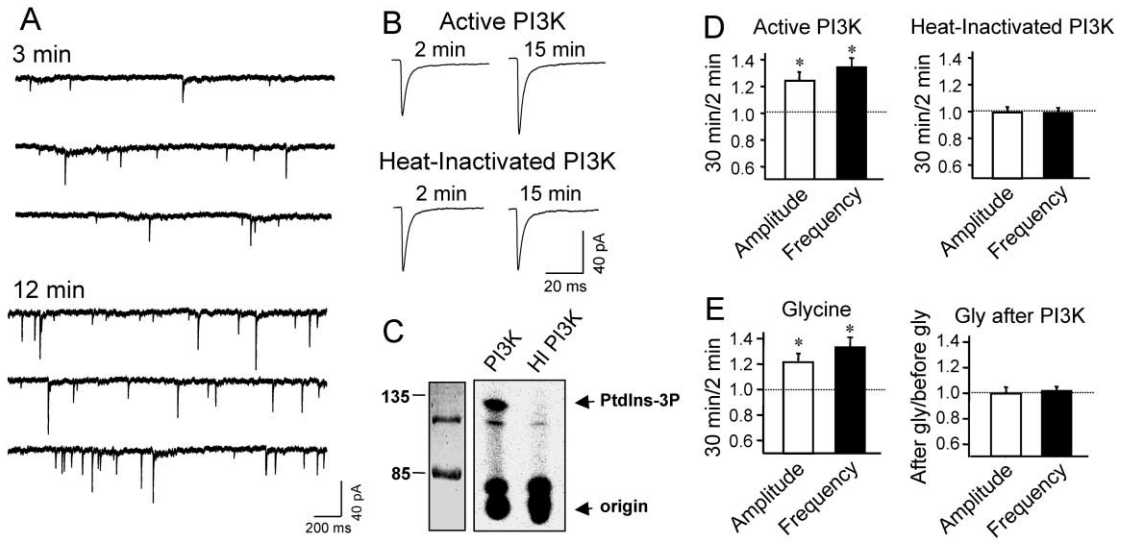

Figure 3. Active PI3K Potentiates mEPSCs and Occludes Glycine-Induced LTP

(A) Continuous traces of mEPSCs taken at the times indicated from a hippocampal neuron recorded with intracellular solution containing active PI3K (1 μg/ml).

(B) Averaged mEPSCs (n = 100 events) taken at 2 and 15 min after the start of whole-cell recordings from two individual neurons recorded, respectively, with active and heat-inactivated, purified PI3K-containing intracellular solutions.

(C) Active PI3K was purified from Sf9 cells infected with recombinant p85α- and p110α-expressing baculovirus. As shown on the Coommassie blue-stained SDS gel (left), the purified complex yielded two bands as expected for the recombinant p85α and p110α subunits of PI3K. Catalytically inactive PI3K was obtained by boiling the purified p85α/p110α complex for 10 min. Lipid kinase activity of active and heat-inactivated PI3K complexes was assayed using exogenous phosphatidylinositol (PtdIns) and ^{32}P-γ-ATP as substrates (see Experimental Procedures). As shown in the autoradiogram on the right, the active but not the heat-inactivated (HI PI3K) PI3K complex phosphorylated PtdIns substrates and generated PtdIns-3*P*.

(D) Plots summarize data from cells recorded with active (Active PI3K; amplitude of 1.25 ± 0.06 and frequency of 1.35 ± 0.07; n = 6) or heat-inactivated PI3K (HI PI3K; 1.01 ± 0.03 and 0.99 ± 0.04; n = 5) in the patch pipettes. The amplitudes and frequencies of mEPSCs at 30 min were normalized to the values from the initial 2 min. Both the amplitudes and frequencies of mEPSCs increased following intracellular application of active but not heat-inactivated recombinant PI3K.

(E) Graphs show the occlusion of glycine-induced LTP of mEPSCs by intracellular pretreatment with PI3K. For cells recorded with active PI3K in the patch pipette (Gly after PI3K), the amplitude and frequency measured 20 min after the start of whole-cell recording, at which point the potentiation of mEPSCs by PI3K had stabilized at its peak value, were normalized to the values 30 min after the glycine application. For the controls (Glycine), glycine was applied at the same time point as the Gly after PI3K group. In the absence of active PI3K in the recording pipette, both mEPSC amplitude and frequency were enhanced (Glycine; 200 μM, 1.23 ± 0.06 and 1.34 ± 0.07; n = 6). However, this enhancement was absent in cells recorded with active PI3K in the patch pipette (Gly after PI3K; 0.99 ± 0.05 and 1.02 ± 0.03; n = 4), which increased both mEPSC amplitude and frequency to a degree similar to glycine application.

live neurons with an antibody against an amino-terminal extracellular epitope of the GluR2 subunit and a cold (non-fluorescence-conjugated) secondary antibody at 4°C. Neurons were then transferred to 37°C to allow the resumption of AMPAR insertion for various periods of time in the presence or absence of glycine and/or PI3K inhibitors. Newly inserted AMPARs were then labeled with the same primary antibody followed by a Cy3-conjugated secondary antibody for fluorescent confocal imaging (Figure 4B) or an HRP-conjugated secondary antibody for cell-ELISA quantification (Figure 4C) under nonpermeant conditions following light fixation. Intracellular AMPARs were subsequently stained with the same primary antibody and FITC- or HRP-conjugated secondary antibody under cell-permeant conditions. The specificity of this method has been characterized previously (see Figure 7B in Lu et al., 2001), and the lack of immunofluorescent staining at time 0 (without switching the cells to room temperature) further confirmed the effective blockade of the preexisting cell surface AMPARs by the cold antibody (Figure 4E). As shown in Figure 4B, 30 min after switching the cells to 37°C, there were newly inserted GluR2-stained clusters on the surface of soma and dendritic trees, representing a rapid, constitutive insertion of AMPARs into the plasma membrane (Lu et al., 2001). As previously reported, most of these GluR2 clusters were colocalized with the synaptic marker synaptophysin, suggesting that some if not all of the receptors were inserted directly at synaptic sites (see Figure 7A in Lu et al., 2001). Treatment with glycine (200 μM; 3 min) produced a dramatic increase in the number of newly inserted GluR2 clusters (Figure 4B). Quantification of the AMPAR insertion using a nonbiased cell-ELISA assay (Figure 4C) demonstrated that glycine treatment resulted in a more than 2-fold increase in newly inserted AMPARs (2.2 ± 0.08; n = 49; $p < 0.05$) and that this increase was prevented when LY294002 (10 μM) was present during and after glycine treatment (0.98 ± 0.05; n = 49; $p > 0.05$). Interestingly, the inhibition by LY294002 of the glycine-induced increase in AMPAR insertion was reversible. Thus, 30 min after washing out LY294002, the level of newly inserted AMPARs on the membrane surface returned to 1.8 ± 0.07 -fold of the control level (n = 49; $p < 0.05$; Figure

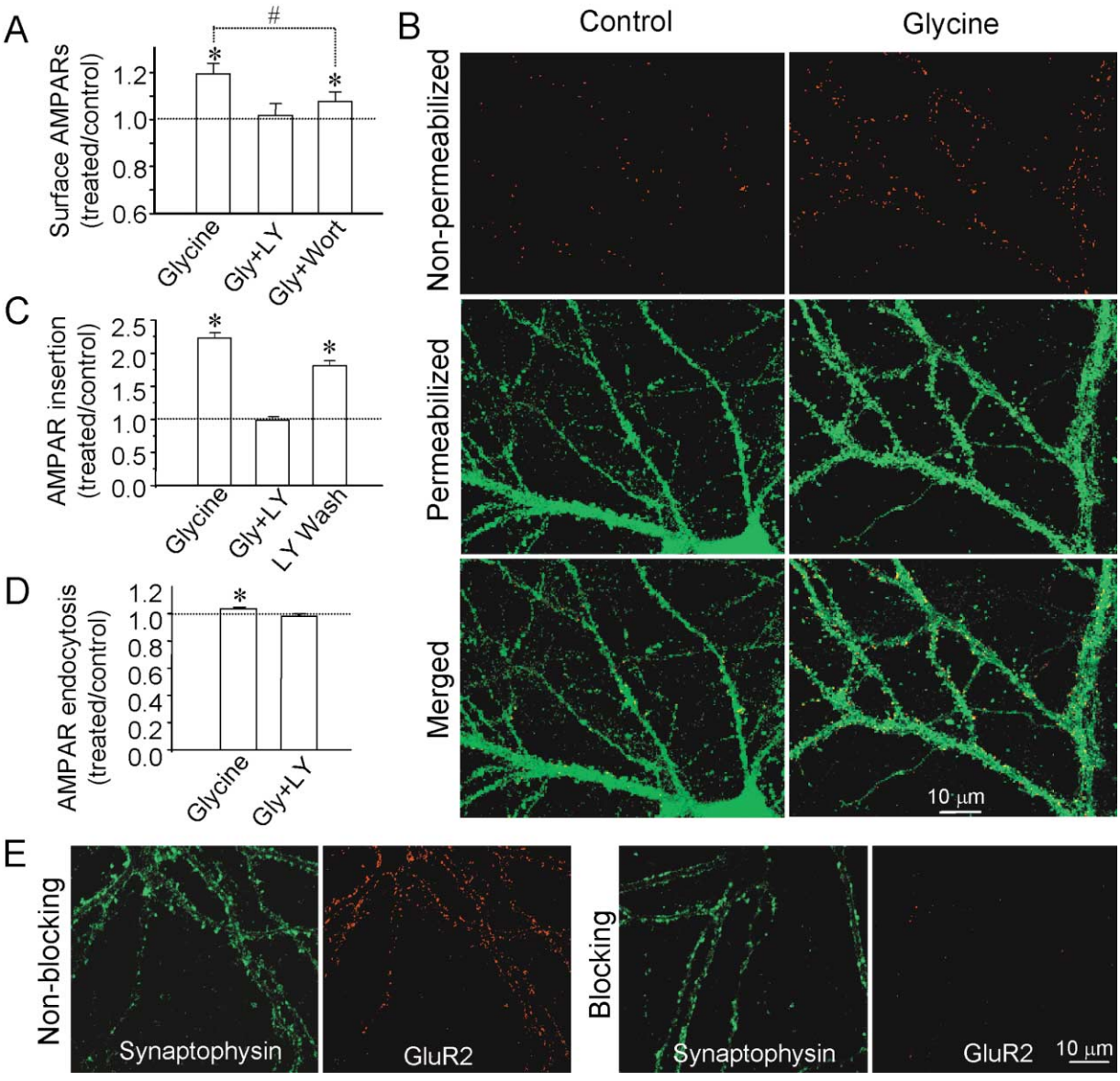

Figure 4. Activation of PI3K Increases Cell Surface Expression of AMPARs by Facilitating Receptor Insertion

(A) Measuring steady-state cell surface AMPARs using colorimetric cell-ELISA assays demonstrates that glycine application results in a rapid increase in the cell surface expression of AMPARs and that this increase is fully blocked by LY294002 (10 μM, n = 6) and partially inhibited by wortmannin (100 nM; n = 6). *$p < 0.05$, comparing with its own control (values before glycine treatment) and #$p < 0.05$, comparing with treatment with glycine alone. (B and C) PI3K is involved in facilitation of AMPAR insertion. After blocking existing cell surface AMPARs with primary antibody recognizing the N-terminal extracellular domain of GluR2 and cold (non-fluorescence-conjugated) secondary antibody, neurons were incubated at 37°C in the absence (Control) or presence of one of the indicated drug treatments for 30 min. The newly inserted cell surface AMPARs were then visualized using confocal microscopy or quantified using a cell-ELISA assay. Example images of newly inserted cell surface (red; nonpermeabilized) and intracellular (green; permeabilized) AMPARs under control (Control) or following glycine treatment (Glycine; 100 μM; 5 min) are shown in (B). Double staining of cells with GluR2 (red; nonpermeabilized) and synaptophysin (green; permeabilized) immediately after preblocking shows that the preblock, while having no effect on synaptophysin staining, essentially eliminated GluR2 labeling (GluR2), confirming the specific and effective blockade of preexisting cell surface AMPA receptors (E). A histogram of the quantification of the glycine-induced increase in AMPAR insertion using the cell-ELISA assay is shown in (C). Glycine facilitated AMPAR insertion (Glycine), and this facilitation was prevented by 10 μM LY294002 (Gly + LY). Moreover, 30 min after LY294002 was washed off the cells (LY Wash), there was a significant recovery of the glycine-induced increase in AMPAR insertion (n = 49). (D) Glycine does not inhibit the AMPAR endocytosis process. The cell surface AMPARs were prelabeled with an antibody raised against an N-terminal extracellular epitope of GluR2 in live neurons at 4°C and allowed to endocytose for varying lengths of time at 37°C. AMPARs remaining on the cell surface and those internalized into the interior of the cells were then quantified using the cell-ELISA assay with HRP-conjugated secondary antibodies under nonpermeant and permeant conditions. The level of AMPAR endocytosis was determined by the specific loss of the prelabeled surface receptors. Glycine treatment did not inhibit but slightly increased AMPAR endocytosis (Glycine; 1.04 ± 0.01 of the control level, n = 49), which was not observed in the presence of LY294002 (Gly + LY; 0.98 ± 0.01).

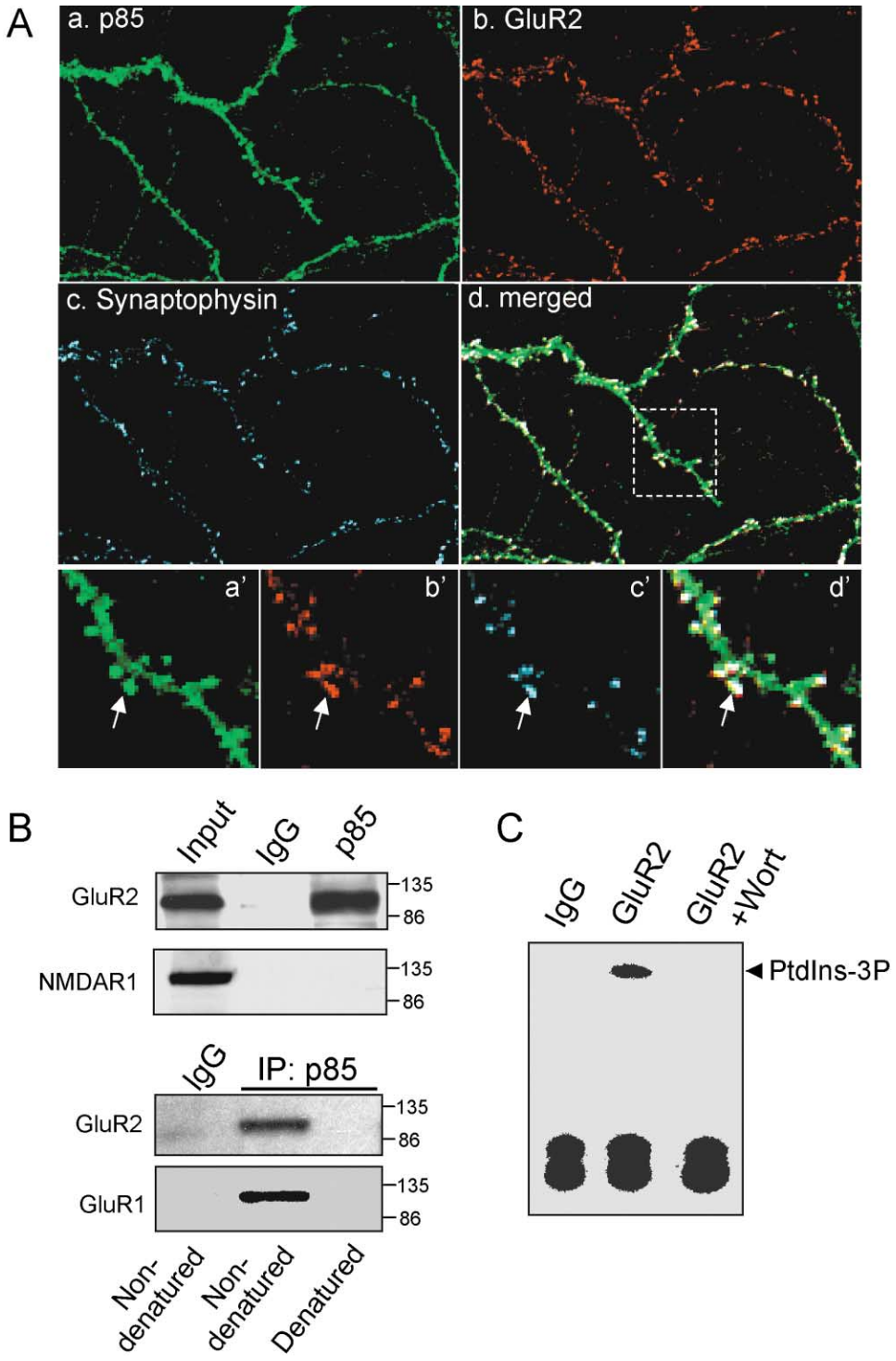

Figure 5. PI3K Is Associated with AMPARs

(A) Colocalization of PI3K with AMPARs in cultured hippocampal neurons. Confocal optical sections of the subcellular distribution of PI3K and AMPARs in the dendrites of a cultured neuron. The p85 subunit of PI3K ([Aa] p85; green) and AMPAR GluR2 subunits ([Ab] GluR2; red) were sequentially stained under permeant conditions. The neurons were then subsequently stained with an antibody against synaptophysin to visualize all synapses ([Ac] Synaptophysin; blue). The superimposed image is shown in (Ad) (merged). The split color channels of the inset indicated in (Ad) were enlarged in panels (Aa′)–(Ad′) and show a high degree of colocalization (see example indicated by the arrows) between PI3K and AMPARs in the dendrites and synapses in punctate clusters near regions stained for synaptophysin, suggesting that the kinase can be compartmentalized to glutamatergic synaptic regions.

(B) PI3K forms a complex with AMPARs in mature brain tissue. (Upper panels) Protein complexes, immunoprecipitated with an anti-p85 antibody from rat hippocampal slice extracts under nondenaturing conditions, were sequentially probed with anti-GluR2 (GluR2) or anti-NMDAR1 (NMDAR1) antibodies. Anti-p85 antibody but not control IgG was able to immunoprecipitate GluR2 but not NMDAR1. (Lower panels)

4C). These results strongly suggest that activation of PI3K is required for glycine-induced facilitation of AMPAR insertion, possibly by being involved at a late step of the receptor insertion process. We next examined the effect of PI3K inhibition on AMPAR endocytosis using a receptor endocytosis assay (antibody-feeding assay) described previously (Lin et al., 2000; Man et al., 2000b). Live neurons were prelabeled with an antibody against extracellular GluR2 at 4°C. The cells were switched to 37°C to allow the resumption of receptor endocytosis, and 30 min later, the prelabeled receptors remaining on the cell surface and those endocytosed into intracellular compartments were detected using a cell-ELISA assay under nonpermeant and permeant conditions, respectively (Man et al., 2000b). As predicted, glycine treatment did not inhibit AMPAR endocytosis but instead resulted in a small but statistically significant facilitation of endocytosis. The facilitation of endocytosis is most likely due to a compensatory response secondary to glycine stimulation of the AMPAR insertion process (Liang and Huganir, 2001; Man et al., 2000b). Consistent with this conjecture, as with the glycine-induced increase in AMPAR insertion (Figure 4C), this facilitation of endocytosis was prevented by LY294002 (Figure 4D). Thus, taken together, our results indicate that glycine stimulation increases the number of cell surface AMPARs in a PI3K-dependent manner and that the increase is primarily the result of facilitated receptor insertion and not due to inhibited receptor endocytosis.

PI3K has been shown to exert diverse biological actions even within the same cell; however, stimulus-dependent specificity of its actions is possible, and in most cases, this specificity is critically dependent upon its compartmentalization with downstream effectors (Heller-Harrison et al., 1996; Yang et al., 1996). We therefore reasoned that the subcellular localization of PI3K activation within the activated synapse might account for the specific involvement of this lipid kinase in the LTP but not the LTD of mEPSCs. To test our hypothesis, we first determined whether PI3K was present in the glutamatergic synapses of cultured hippocampal neurons using immunofluorescent confocal microscopy. PI3K was first labeled in cultured neurons with an antibody against the p85 subunit, and the same neurons were subsequently stained for postsynaptic AMPAR GluR2 subunits in order to identify glutamatergic synapses. As a final step, all synapses on the hippocampal neurons were detected via staining for synapse-specific synaptophysin. As shown in Figure 5A, PI3K was localized throughout the neurons, including in dendrites. Notably, within the dendrites PI3K was not uniformly distributed but was found in numerous small clusters and in what appeared to be spines (panel inset in Figure 5Aa′). The majority of these dendritic PI3K punctae were colocalized with AMPAR GluR2 subunits at synapses as shown in the overlay panel (also see inset in Figure 5Ad′ of the overlay panel). These staining results suggest that PI3K and AMPARs can colocalize in discrete punctate regions and that many of these are localized near synapses.

One potential mechanism by which PI3K could be compartmentalized at glutamatergic synapses is through association with synaptically localized proteins, such as glutamate receptors themselves and/or their clustering proteins. We therefore immunoprecipitated PI3K from rat hippocampal lysates using an antibody against the p85 subunit under nondenaturing conditions and then sequentially probed the immunoprecipitated protein complex using antibodies against either GluR2 subunits or the NMDAR NR1 subunit in order to investigate whether PI3K is associated with either NMDARs or AMPARs. As shown in Figure 5B, AMPA (both GluR1 and GluR2 subunits) but not NMDA receptors were specifically coimmunoprecipitated with PI3K under nondenaturing conditions. The immunoprecipitation of AMPAR subunits was not seen with control IgG, nor when the samples were boiled for 5 min (to dissociate protein complexes) prior to the immunoprecipitation. Thus, PI3K appears to complex with AMPARs in hippocampal neurons. The failure to coimmunoprecipitate NMDARs with PI3K is surprising, as a previous study reported an association of PI3K with these receptors via a direct interaction between the tyrosine phosphorylated NR2B subunit and p85 (Hisatsune et al., 1999). One potential explanation is that the level of endogenous tyrosine phosphorylation of NMDARs under our experimental conditions was too low to support such a tyrosine phosphorylation-dependent complex formation. To further determine whether the PI3K complexed with AMPARs was functional, we coimmunoprecipitated PI3K using an anti-GluR2 antibody, and measured the ability of the AMPAR-associated PI3K to form PtdIns 3-*P* from PtdIns and ^{32}P-γ-ATP (Figure 5C). This immunocomplex/lipid kinase assay revealed that GluR2 antibodies were able to precipitate PI3K activity, whereas control IgG was not. Preincubation with wortmannin completely blocked the AMPAR-associated PI3K activity. These results not only confirm that PI3K is associated with AMPARs in hippocampal neurons in situ, but also demonstrate that the receptor-kinase complex is functionally active.

The receptor-kinase complex could form directly, by interaction between the AMPAR and PI3K, or indirectly, with the aid of a bridging protein(s). To determine whether or not the PI3K-AMPAR association is mediated by a direct interaction, we performed an in vitro recombinant protein binding assay. Native AMPARs are likely heterooligomeric complexes assembled from GluR1-4 subunits, and the most common subunit combinations of native AMPARs in hippocampal CA1 neurons are

Sequential immunoblotting for GluR2 and GluR1 shows that both subunits are present in p85 immunoprecipitated complexes and that boiling the samples for 5 min (to denature protein complexes) prior to the immunoprecipitation eliminated the ability of the anti-p85 antibody to coimmunoprecipitate either GluR2 or GluR1.

(C) PI3K in the AMPAR complex is functional. PI3K assays were performed on protein complexes immunoprecipitated with anti-GluR2 antibody under nondenaturing conditions. Anti-GluR2 antibody but not the control IgG was able to immunoprecipitate lipid kinase activity (see arrowhead for kinase reaction product), which was completely abolished by the addition of the PI3K inhibitor wortmannin in the kinase assay buffer (Wort; 100 nM; 10 min).

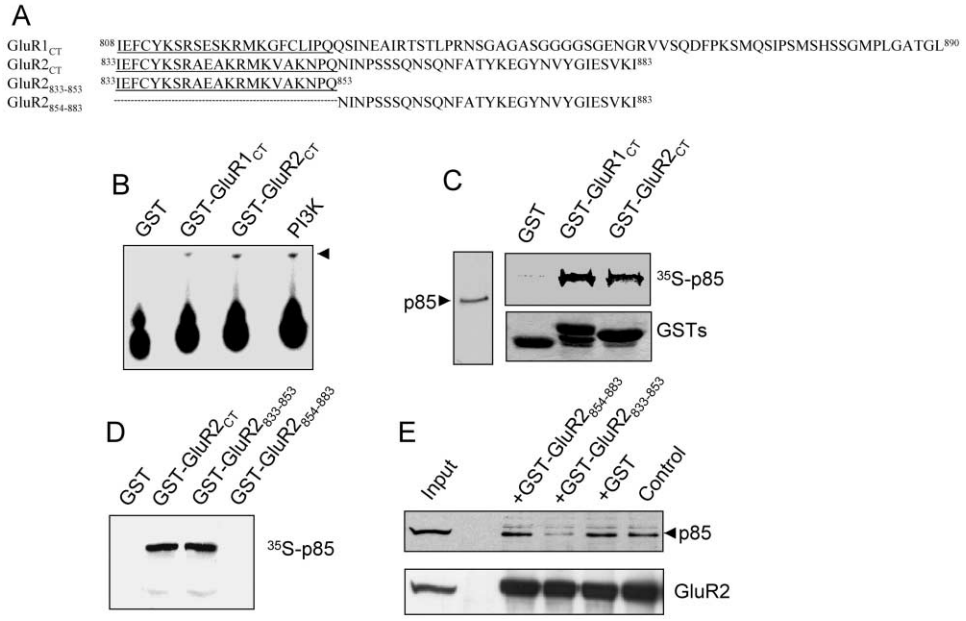

Figure 6. Direct Interaction between PI3K and AMPAR

(A) Sequence alignments of GST constructs containing the carboxyl tails of GluR1 and GluR2. The highly conserved region among all GluR subunits is underlined.

(B) Both GluR1 and GluR2 interact with PI3K (p85/p110) complex in vitro. The purified active recombinant PI3K complex (p85/p110; see Figure 3C) was incubated with GST or GST fusion proteins containing either GluR1 (GST-GluR1$_{CT}$) or GluR2 (GST-GluR2$_{CT}$) carboxyl tail, and the affinity precipitates, along with purified PI3K (PI3K) as a positive control, were then subjected to a PI3K activity assay. Both GST-GluR1$_{CT}$ and GST-GluR2$_{CT}$ but not GST alone were able to bind and, hence, precipitate the PI3K complex.

(C) The p85 subunit of PI3K binds to GST-GluR1$_{CT}$ and GST-GluR2$_{CT}$ in vitro. The p85 subunit of PI3K was in vitro translated and radioactively labeled with [^{35}S]methionine. The autoradiogram on the left shows that the reaction produced a single protein band with a molecular weight corresponding to the p85 subunit. (Right) The in vitro translated p85 was then incubated with GST, GST-GluR1$_{CT}$, or GST-GluR2$_{CT}$, and the precipitates were subjected to SDS-PAGE. Autoradiography shows that both GST-GluR1$_{CT}$ and GST-GluR2$_{CT}$ but not GST alone precipitate the p85 subunit (top). A Coommassie blue-stained gel (bottom) indicates that a similar amount of GST fusion protein was used in each of the precipitation experiments.

(D) Autoradiogram shows that GST fusion protein containing the first 21 amino acids of the GluR2 CT (GST-GluR2$_{833–853}$, the conserved region) but not GST fusion protein containing the last 30 amino acids of the GluR2 CT (GST-GluR2$_{854–883}$) nor GST alone was capable of precipitating the p85 subunit.

(E) Direct interaction between p85 and GluRs is responsible for the complex formation between PI3K and AMPARs in mature neurons in situ. Hippocampal lysates were immunoprecipitated with anti-GluR2 antibody in the absence (Control) or presence of one of the GST fusion proteins (50 μg) under nondenaturing conditions, and the immunoprecipitates were then separated on SDS-PAGE and sequentially probed for p85 and GluR2. GST-GluR2$_{833–853}$ but not GST-GluR2$_{854–883}$ nor GST alone inhibited the ability of anti-GluR2 antibody to coimmunoprecipitate p85. Result represents one of two replicates.

GluR1/GluR2 and GluR2/GluR3 (Wenthold et al., 1996). In addition, several intracellular proteins associate with AMPARs via their binding to the cytoplasmic carboxyl tails (CTs) of GluRs (Kim and Huganir, 1999; Sheng and Sala, 2001). We therefore incubated purified recombinant p85α/p110α PI3K with GST fusion proteins containing the CT of GluR1 (GST-GluR1$_{CT}$) or GluR2 (GST-GluR2$_{CT}$) subunits and assayed whether these fusion proteins could specifically affinity precipitate the PI3K complex as measured by PI3K activity in the precipitates. As shown in Figure 6, both GST-GluR1$_{CT}$ and GST-GluR2$_{CT}$ but not GST alone were able to precipitate active PI3K, supporting the interpretation of direct binding between the PI3K complex and these GluR CTs. The p85α regulatory subunit of PI3K contains multiple protein-protein interaction motifs (Vanhaesebroeck et al., 1997). Therefore, we hypothesized that this subunit directly binds to regions of the GluR CT. Consistent with this hypothesis, we found that both GST-GluR1$_{CT}$ and GST-GluR2$_{CT}$ could specifically precipitate in vitro-translated, [^{35}S]methionine-labeled p85 subunits using an affinity precipitation assay (Figure 6C). Since there is a short amino acid stretch at the N-terminal end of the CT (membrane proximal region) that is highly conserved among all GluR subunits, we suspected that it was this conserved region that was involved in the interaction between PI3K and GluRs. We therefore created two additional GST-GluR2$_{CT}$ fusion proteins, GST-GluR2$_{833–853}$ and GST-GluR2$_{854–883}$ (Figure 6A). The former includes the membrane proximal conserved region, the latter does not. Consistent with our predictions, GST-GluR2$_{833–853}$ but not GST-GluR2$_{854–883}$ was able to interact with p85 (Figure 6D). To further determine whether the identified direct binding is the primary mechanism responsible for complex formation between native AMPAR and PI3K detected by coimmunoprecipitation shown in Figure 5, we performed immunoprecipitation of hippocampal lysate with anti-GluR2 antibody in the presence of GST alone, GST-GluR2$_{833–853}$, or GST-GluR2$_{854–883}$. As shown in the blots in Figure 6E, the GST-GluR2$_{833–853}$ but neither

GST alone nor GST-GluR2$_{854–883}$ drastically reduced the amount of p85 present in the immunoprecipitates. The reduction in p85 was not associated with a notable alteration of GluR2 in the immunoprecipitates. Thus, the GST-GluR2$_{833–853}$ that contains the binding motif for p85 was able to compete with native AMPARs for the binding of endogenous p85, thereby inhibiting complex formation between PI3K and AMPARs. The GluR2$_{833–853}$ region appears to be both necessary and sufficient for mediating GluR-p85 binding and, therefore, AMPAR and PI3K association in situ.

The association of PI3K and AMPARs puts this kinase in a strategic position to mediate the facilitated insertion of these receptors during glycine-induced LTP. It has recently been demonstrated that calmodulin can bind to and activate PI3K in a Ca^{2+}-dependent manner (Joyal et al., 1997). As AMPARs and NMDARs coexist in postsynaptic membranes of glutamatergic synapses, we reasoned that the AMPAR-PI3K interaction might compartmentalize PI3K near NMDAR channels. Since activation of synaptic NMDARs can lead to a localized and transient rise in intracellular Ca^{2+} concentrations ($[Ca^{2+}]_i$) within the activated postsynaptic dendritic spines, this molecular arrangement would allow the selective stimulation of the AMPAR-associated PI3K complex only at those activated synapses where an NMDAR-dependent influx of Ca^{2+} was induced. We examined this possibility by measuring the PI3K activity of AMPAR-kinase complexes immunoprecipitated from hippocampal slices pretreated with or without different glutamate receptor agonists or glycine. As a control, and in parallel, the activity of the entire cellular pool of PI3K from these slices was also measured via immunoprecipitation with an anti-p85 antibody. Consistent with our hypothesis, bath application of glycine (200 μM for 5 min) resulted in a more than 2-fold increase in the PI3K activity associated with the anti-GluR2, but not the anti-p85, immunocomplex (Figures 7A and 7B), and this increase was the result of synaptic activation of NMDARs as the glycine effect was blocked by APV (50 μM). Surprisingly, bath application of neither NMDA (50 μM), which activates both synaptic and extrasynaptic NMDARs and produces LTD of mEPSCs (Lu et al., 2001), nor AMPA (50 μM) notably altered either anti-GluR2 or anti-p85 immunoprecipitated PI3K activity (Figures 7A and 7B). This glycine-induced increase in AMPAR-associated PI3K activity appears to be the result of the activation of the kinase and not due to an increased association between the AMPAR and PI3K, as there was no detectable alteration in the ability of anti-GluR2 to coimmunoprecipitate p85 from slices treated with glycine (Figure 7C; 106.1% $\pm$ 30.1% of control; $n = 8$; $p > 0.05$). Consistent with the requirement for physical association between AMPAR and PI3K in the ability of GluR2 antibody to immunoprecipitate the PI3K activity, incubation of the slice lysates prior to immunoprecipitation with GST-GluR2$_{833–853}$ but not GST-GluR2$_{854–883}$ reduced PI3K activity in the GluR2 immunocomplex of glycine-treated slices to a level even lower than that in control slices (Figure 7D). As shown in Figure 7E, a similar activation of AMPAR-associated PI3K activity by glycine could also be demonstrated in cultured hippocampal neurons following the same glycine stimulation protocol that produced LTP of mEPSCs (Figure 1) and increased plasma membrane AMPAR insertion (Figure 4). Collectively, these results strongly suggest that AMPAR-PI3K interaction leads to the compartmentalization of PI3K in the postsynaptic domain of the glutamatergic synapse, thereby enabling the stimulation of the lipid kinase by synaptic NMDAR activation. These results also correspond well with our electrophysiological results demonstrating the specific requirement for PI3K in glycine-induced LTP (Figure 1), but not in NMDA-induced LTD, of mEPSCs (Figure 2).

Discussion

Our data presented here demonstrate that PI3K is associated with AMPARs and is thereby compartmentalized within the excitatory synapses of hippocampal neurons. Activation of synaptic NMDARs with glycine specifically stimulates the AMPAR-associated PI3K. In addition, we demonstrate that activation of PI3K plays an indispensable role in the glycine-induced facilitation of the insertion of postsynaptic AMPARs and, hence, LTP of mEPSCs. Moreover, we found that the prevention of facilitated AMPAR insertion by inhibiting PI3K activity could be reversed upon removal of the PI3K inhibitor. These results are in good agreement with recently reported involvement of PI3K in mediating the expression but not the induction and maintenance of hippocampal CA1 LTP in slice preparations (Sanna et al., 2002). Together, our results strongly suggest that PI3K is required for facilitated AMPAR insertion, making it a critical molecule that is directly involved in mediating the later step of LTP.

Through our in vitro recombinant protein binding assays, we identified a direct interaction between the membrane proximal region of the CTs of GluR subunits and the p85 subunit of PI3K. Since the short peptide containing this binding region dramatically inhibits the coimmunoprecipitation of PI3K protein (Figure 6E) and activity (Figure 7D) with AMPARs, it is likely that the identified direct binding is the primary determinant that mediates complex formation between PI3K and AMPARs in neurons. It is interesting that this required region is largely conserved among all GluR subunits identified thus far. This implies that the association between AMPARs and PI3K is not a subunit-specific phenomenon but is common to all native AMPARs, underscoring the physiological importance of the association. It is interesting to note that several laboratories have provided evidence supporting an obligatory role of the GluR1 CT in mediating NMDAR-mediated, activity-dependent AMPAR insertion (Hayashi et al., 2000; Passafaro et al., 2001) or hippocampal CA1 LTP (Zamanillo et al., 1999). In particular, Passafaro et al. have recently reported that, in cultured hippocampal neurons, glycine or NMDA stimulation facilitates the plasma membrane insertion of transiently expressed recombinant GluR1 but not GluR2 in a PI3K-dependent manner (Passafaro et al., 2001). Since PI3K can potentially bind to all GluR subunits, the PI3K-dependent and GluR1-specific AMPAR insertion during LTP expression could not be solely explained by the direct binding between PI3K and GluR subunits. In other words, in addition to the PI3K-AMPAR interaction identified here, a GluR1 subunit-dependent process that is either up- or downstream of

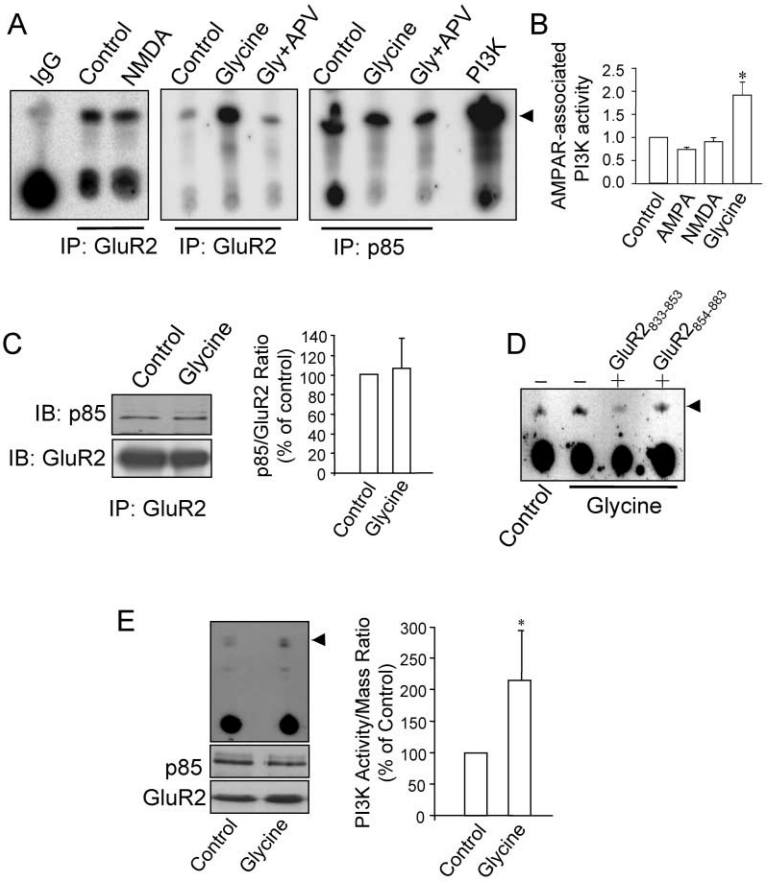

Figure 7. AMPAR-Associated PI3K Is Activated by Selective Stimulation of Synaptic NMDARs

Hippocampal slices were treated with either NMDA (50 μM), AMPA (50 μM), glycine (200 μM), or glycine (200 μM) + APV (50 μM). Tissue homogenates from drug-treated slices or slices without any drug treatment (Control) were then immunoprecipitated with either anti-GluR2 or anti-p85 antibodies or control IgG. The immunocomplexes, along with purified, active PI3K as a positive control (PI3K), were subjected to the PI3K activity assay.

(A) NMDA treatment has little effect on PI3K activity in the AMPAR immunocomplex (IP: GluR2), whereas the activity of AMPAR-associated PI3K is dramatically increased in slices treated with glycine. Moreover, the glycine-induced enhancement of PI3K activity is blocked by coapplication of NMDAR antagonist APV (Gly + APV). In contrast, glycine stimulation did not alter the activity of the total cellular pool of PI3K that was immunoprecipitated with anti-p85 antibody (IP: PI3K).

(B) Summary of the changes in AMPAR-associated PI3K. PI3K activity was normalized by taking the values of the autoradiographic density of their own internal untreated controls as 1 ($n = 3–5$ experiments).

(C) Glycine treatment does not affect the PI3K-AMPAR association. Western blots sequentially probed with anti-p85 and anti-GluR2 antibodies (IB: p85 and GluR2) show there is no obvious alteration in the ability of anti-GluR2 antibody (IP: GluR2) to coimmunoprecipitate p85 in slices treated with or without glycine (200 μM). An amount of p85 was quantified by normalizing the intensity of the p85 band to that of GluR2 and expressed as percentage of control levels in the graph on the right ($n = 8$; $p > 0.05$).

(D) Glycine-induced increase in AMPAR-associated PI3K activity requires direct interaction between p85 and GluRs. Hippocampal lysates from control (Control) and glycine (Glycine)-treated slices were immunoprecipitated with anti-GluR2 antibody in the absence (−) or presence (+) of one of the GST fusion proteins (50 μg) under nondenaturing conditions, and the immunoprecipitates were then subjected to the PI3K activity assay. GST-$GluR2_{833–853}$ ($GluR2_{833–853}$) but not GST-$GluR2_{854–883}$ ($GluR2_{854–883}$) nor GST alone inhibited the ability of anti-GluR2 antibody to coimmunoprecipitate PI3K activity. Autoradiogram is representative of two replicates.

(E) Glycine stimulated AMPAR-associated PI3K activity in cultured hippocampal neurons. (Left) PI3K was coimmunoprecipitated with anti-GluR2 antibody from tissue homogenates of control hippocampal cultures (Control) or cultures treated with glycine (Glycine; 200 μM; 3 min), and the immunoprecipitates were then subjected to either PI3K activity assay (top panel) or sequential Western blotting (bottom panels: p85 and GluR2). (Right) PI3K activity was quantified by normalizing the PI3K activity to the amount of immunoprecipitated p85 (PI3K activity/mass ratio) and expressed as percentage of controls.

the PI3K activation may also be involved in mediating subunit-specific AMPAR insertion during LTP.

One well-characterized feature of LTP is the input or synapse specificity, i.e., synaptic plasticity is only exhibited in activated synapses. Transient rises in intracellular Ca^{2+} within the activated synaptic spine region as a consequence of Ca^{2+} influx through the activated NMDARs have been suspected to be one of the major mechanisms mediating this synaptic specificity (Bliss and Collingridge, 1993; Malenka and Nicoll, 1999). However, the signaling molecules activated directly by these intrasynaptic rises in $[Ca^{2+}]_i$ remain unidentified. Two unique features associated with PI3K make the AMPAR-associated PI3K complex one of the most attractive candidate molecules for the link between activation of synaptic NMDARs and the production of LTP. First, through its association with AMPARs, PI3K is compartmentalized within the postsynaptic density of glutamatergic synapses and hence is recruited to the vicinity of synaptic NMDARs. As a result, the AMPAR-associated PI3K complex is in a strategic location to "sense" the localized rises in Ca^{2+} concentrations resulting from the gating of NMDAR channels, and it provides a synapse-selective detector for the production of LTP. The second unique feature of PI3K, with regard to its candidacy as a mediator of LTP input specificity, comes from its lipid products. Unlike most diffusible cytosolic second messengers, once produced, PtdIns-3Ps remain in the membrane, thereby ensuring that the activated signaling cascades that lead to LTP are restricted to activated synapses.

PI3K is known to be activated by complexed Ca^{2+} and calmodulin (Joyal et al., 1997). NMDAR activation causes a localized rise in Ca^{2+} sufficient to form a Ca^{2+}-calmodulin complex. This complex can potentially activate the AMPAR-associated PI3K, thereby mediating specific AMPAR insertion within these activated synapses. However, the NMDAR-dependent increase in

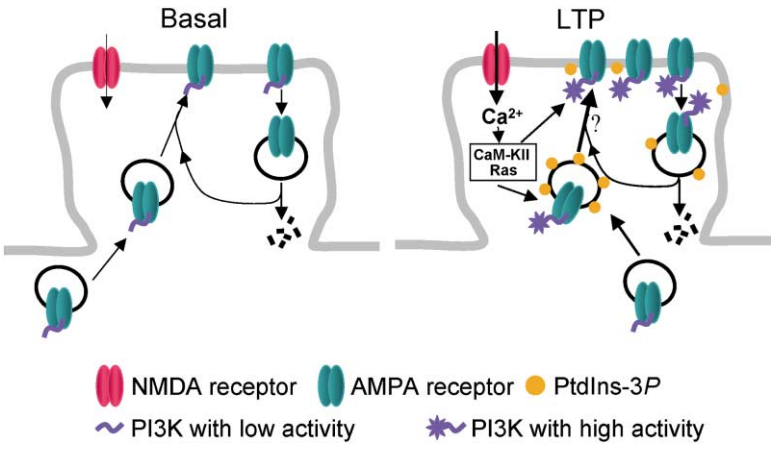

Figure 8. Proposed Role of AMPAR-Associated PI3K in LTP

We tentatively speculate that there is a reserve pool of AMPAR-containing vesicles within the dendritic spines or in their vicinity. Under basal conditions, these vesicles are constitutively inserted into synaptic plasma membranes at a relatively slow rate to counteract a slow constitutive AMPAR endocytosis, thereby ensuring a constant number of postsynaptic AMPARs (Liang and Huganir, 2001; Man et al., 2000b). Following LTP stimulation protocols, Ca^{2+} influx through the activated NMDARs results in a transient and localized rise in $[Ca^{2+}]_i$ within the activated synapses. Once the $[Ca^{2+}]_i$ is sufficient, there is a sequential translocation and activation of CaM-KII (Bayer et al., 2001; Shen and Meyer, 1999) and Ras (Zhu et al., 2002) within these synapses. Ras then activates AMPAR-associated PI3K (Downward, 1997; Rodriguez-Viciana et al., 1996), resulting in the production and accumulation of membrane binding PtdIns-3Ps within the activated synapses. PtdIns-3Ps, in turn, facilitate membrane fusion of AMPAR-containing vesicles with the plasma membrane through uncharacterized mechanisms ("?," by affecting membrane properties or recruitment of other molecules such as kinases implicated in LTP), resulting in the insertion of the receptors at activated synapses during the expression phase of LTP. For the sake of clarity, the endocytotic arm of AMPAR trafficking, along with a large number of molecules previously implicated in LTP expression, have been omitted.

$[Ca^{2+}]_i$ is transient and only occurs during the induction period of LTP, while the PI3K-dependent facilitation of AMPAR insertion is maintained throughout the expression period. Thus, how such a transient rise in $[Ca^{2+}]_i$ is translated into a long-lasting signal responsible for sustained activation of PI3K and, hence, the facilitated insertion of AMPARs remains to be elucidated. In view of this, it is very interesting to note that activation of NMDARs has been demonstrated to be able to recruit and activate the serine/threonine kinase CaM-KII to these synapses (Shen and Meyer, 1999). Once activated, the kinase is believed to be locked in the activated state (Bayer et al., 2001; Lisman et al., 2002). This activation has been proposed as one of the important mechanisms that maintain facilitated AMPAR insertion during LTP; how the lasting activation of CaM-KII leads to a maintained increase in AMPAR insertion remains unclear. As mutation of the CaM-KII phosphorylation site in the GluR1 CT did not prevent the synaptic delivery of AMPARs, direct phosphorylation of GluR1 by CaM-KII may not be a critical event leading to facilitated AMPAR insertion (Hayashi et al., 2000). Zhu et al. have recently provided strong evidence suggesting that CaM-KII may facilitate AMPAR insertion by activating Ras (Zhu et al., 2002). In light of this, it is significant to note that Ras is known to activate PI3K by mechanisms including a direct interaction with the catalytic subunit of the lipid kinase (Downward, 1997; Rodriguez-Viciana et al., 1996). Thus, we can tentatively propose, as illustrated in Figure 8, that selective activation of synaptic NMDARs may lead to a transient rise in $[Ca^{2+}]_i$ localized within the activated synapses, which in turn recruits and activates CaM-KII and Ras. Ras then binds and activates AMPAR-associated PI3K, leading to lasting facilitation of AMPAR insertion. In this model, NMDAR activation and a transient increase in $[Ca^{2+}]_i$ in the activated synapses is a critical signal involved in mediating the induction of LTP within these synapses, while the activation of CaM-KII/Ras and subsequent activation of AMPAR-associated PI3K are responsible for the maintenance and expression (AMPAR insertion) of LTP, respectively.

Accumulating evidence suggests that enhanced synaptic insertion of AMPARs into the postsynaptic plasma membrane, via exocytosis of AMPAR-containing vesicles, is an important postsynaptic mechanism in the expression of a number of forms of NMDAR-dependent LTP (Lu et al., 2001; Malinow et al., 2000; Passafaro et al., 2001; Shi et al., 1999). In addition, PI3K has also been implicated in some forms of synaptic plasticity, although the underlying mechanisms remain to be characterized (Kelly and Lynch, 2000; Lin et al., 2001). PtdIns-3Ps are known to be important signaling molecules involved in many membrane trafficking processes (Carpenter and Cantley, 1996; Cheever et al., 2001; De Camilli et al., 1996; James and Piper, 1994; Rapoport et al., 1997), and our results are consistent with activation of the AMPAR-associated PI3K complex, following the selective activation of synaptic NMDARs. The accumulation of PI3K products near AMPAR-containing vesicles might then directly or indirectly stimulate localized plasma membrane insertion of AMPARs only at activated synapses. The mechanism by which such a synaptic accumulation of PtdIns-3Ps facilitates AMPAR insertion into these synapse membranes during LTP remain to be established. In this respect, it has been shown in yeast that PtdIns-3Ps recruit tSNARE Vam7, via their PX binding domains, to PtdIns-3P-enriched vacuoles and thereby facilitate the docking and fusion of transport intermediates with the vacuole (Cheever et al., 2001). Thus, one possibility is that accumulation of PtdIns-3Ps in the vicinity of AMPAR-containing vesicles may affect the physical properties of the postsynaptic plasma membrane and/or the membrane of the AMPAR-containing vesicles in these synapses and consequently prime or facilitate the fusion process between the two membranes. In addition, PtdIns-3Ps are known to specifically bind other protein modules such as PH and FYVE domains (Stenmark and Aasland, 1999). It is possible that accumulation of PtdIns-3Ps around the AMPAR-containing vesicles recruits a PtdIns-3P binding module-containing signaling complex, such as the serine/threonine kinases PKC and Akt (Vanhaesebroeck et al.,

1997), to activated synapses, thereby creating localized signaling cascades responsible for insertion of AMPARs into the plasma membrane at these synapses during the expression of LTP. Therefore, identifying the molecules immediately downstream of the AMPAR-associated PI3K complex [i.e., the effector(s) of PtdIns-3Ps] should facilitate our efforts in understanding the molecular mechanisms underlying LTP.

Experimental Procedures

mEPSCs in Neuronal Cultures

Cultured mouse hippocampal neurons were grown as previously described (Lu et al., 2001). Whole-cell recordings were made from these cultures 12–17 days after plating. Patch electrodes were coated with Sylgard to improve signal-to-noise ratios. Recordings were performed at room temperature (20°C–22°C). Recordings from each neuron lasted for at least 40–80 min. Recordings where the series resistance varied by more than 10% were rejected. No electronic compensation for series resistance was employed. The intracellular recording (patch electrode) solution contained (in mM) $CsCl_2$, 140; EGTA, 2.5; $MgCl_2$, 2; HEPES, 10; TEA, 2; K_2ATP, 4; plus or minus active or heat-inactivated PI3K (1 μg/ml); at pH 7.3 and osmolarity 300–310 $mosmol^{-1}$. The extracellular recording solution (ECS) consisted of (in mM) NaCl, 140; $CaCl_2$, 1.3; KCl, 5.0; HEPES, 25; glucose, 33; TTX, 0.0005; strychnine, 0.001; bicuculline methiodide, 0.02; at pH 7.4 and osmolarity 325–335 $mosmol^{-1}$. Each cell was continuously superfused (1.0 ml/min) with the extracellular solution from a single barrel of a computer-controlled multi-barreled perfusion system. Solutions supplemented with glycine or glycine and NMDA were applied from an alternate barrel. mEPSCs were recorded using an Axopatch 1-B amplifier (Axon Instruments Inc., Union City, CA), and records were filtered at 2 kHz, stored on tape, and subsequently acquired offline with an event detection program (SCAN, Strathclyde software, courtesy of Dr. J. Dempster). The trigger level for detection of events was set approximately three times higher than the baseline noise. Inspection of the raw data was used to eliminate any false events.

Immunocytochemisty

Immunocytochemistry was performed essentially as previously reported (Man et al., 2000b). For colocalization, cultured hippocampal neurons were washed briefly with D-PBS and then fixed for 10 min with 4% paraformaldehyde in D-PBS without cell permeabilization. Neurons were then blocked in 10% normal goat serum in D-PBS prior to overnight incubation with 1:1000 mouse monoclonal antibody recognizing the N-terminal extracellular domain of GluR2 (anti-GluR2, Chemicon International, Inc., Temecula, CA) and with Cy5 conjugated anti-mouse secondary antibodies. Neurons were then permeabilized with 0.1% Triton in D-PBS for 5 min and incubated for 1 hr at room temperature with a rabbit polyclonal antibody against the p85 subunit of PI3K at a dilution of 1:1000 (Upstate Biotechnology, Lake Placid, NY) and FITC conjugated anti-rabbit antibodies. Following extensive washes, the neurons were incubated again with a goat polyclonal antibody against synaptophysin (1:1000, Santa Cruz Biotechnology Inc., Santa Cruz, CA) and a Cy3 conjugated anti-goat antibody for 1 hr at room temperature. Neurons were washed extensively and then mounted prior to imaging on a Zeiss LSM510 confocal microscope. Methods for confocal fluorescent microscopic visualization of newly inserted AMPARs have been previously described (Lu et al., 2001). In brief, live hippocampal cells were first incubated with the monoclonal anti-GluR2 antibody (1:500; Chemicon International, Inc.) for 45 min and a cold (nonconjugated) secondary antibody (5 μg/mL; Sigma, St. Louis, MO) for another 45 min at 4°C to block the preexisting cell surface AMPARs. Following treatments at 37°C for various times as detailed in the text and the legend of Figure 4, the cells were fixed and stained with the same anti-GluR2 primary antibody and Cy3-conjugated anti-mouse secondary antibody to detect the newly inserted AMPARs on the plasma membrane surface. The cells were then permeabilized with 0.1% Triton X-100 in PBS for 5 min, rinsed thoroughly with PBS and then stained for intracellularly localized AMPARs using the same anti-GluR2 antibody and an FITC-conjugated anti-mouse secondary antibody. The images were acquired using a 63× objective lens on a Zeiss confocal microscope (1024 × 1024 pixels).

Cell-ELISA Assays

The measurement of the steady-state level of cell surface AMPARs (cell surface receptor assays) were performed as described previously (Man et al., 2000b). In brief, cultured hippocampal neurons were treated with glycine (200 μM), with or without PI3K inhibitors LY294002 (10 μM) or wortmannin (100 nM), in the perfusion solution for 3–5 min and then allowed to recover in perfusion solution (without glycine) for 15–20 min. Following 10 min fixation with 2% paraformaldehyde and, for some cells, permeabilization with 0.2% Triton X-100 in PBS for 10 min, neurons were labeled with a polyclonal antibody against the N-terminal extracellular domain of the rat GluR1 receptor (Oncogene Research, 1:100) and a horseradish peroxidase (HRP)-conjugated anti-rabbit secondary antibody (1:1000). Cells were washed five times with PBS to minimize nonspecific reactivity then they were incubated with 1 ml of HRP substrate OPD (Sigma) for 2–5 min. Reactions were stopped with 0.2 ml 3 N HCl, and the optical density of the supernatant was read on a spectrophotometer at 492 nm. The levels of cell surface expression of AMPARs were presented as the ratio of colorimetric readings under nonpermeabilized conditions to those under permeabilized conditions and were normalized to untreated control values.

For quantification of AMPAR insertion using cell-ELISA (AMPAR insertion assay [Lu et al., 2001]), cell surface AMPARs were first blocked with anti-GluR2 antibody and a non-HRP conjugated secondary antibody as described above in the immunocytochemistry section, and newly inserted AMPARs were then labeled with the same primary antibody and an HRP-conjugated secondary antibody under nonpermeabilized conditions followed by detection with HRP-OPD reactions. The entire cellular pool of AMPARs was assayed using the same method under permeabilized conditions. The level of insertion was then determined by taking the ratio of readings under nonpermeant over permeant conditions. For quantification of AMPAR endocytosis using cell-ELISA (AMPAR endocytosis assay [Lu et al., 2001; Man et al., 2000b]), live cells were incubated with the anti-GluR2 antibody recognizing the N-terminal extracellular domain at 4°C to prelabel cell surface AMPARs. Following treatments at 37°C for various times as indicated in the text and the legend of Figure 4D, cells were respectively labeled with HRP-conjugated secondary antibody under nonpermeant (to detect prelabeled receptors that remained on the cell surface) and permeant conditions (to detect prelabeled receptors that had been endocytosed into the cell interior), followed by detection with HRP-OPD as described above. Levels of AMPAR endocytosis were then determined by the ratio of colorimetric readings under nonpermeabilized and permeabilized conditions and were normalized to untreated control values.

GST Fusion Proteins and Affinity Precipitations

$pGEX2T\text{-}GluR1_{CT}$ and $pGEX2T\text{-}GluR2_{CT}$ plasmids were gifts from Morgan Sheng (Harvard Medical School). Corresponding GST fusion proteins were produced and purified from bacterial lysates using procedures suggested by the manufacturer (Amersham Biosciences, Baie d'Urfé, PQ). Active recombinant PI3K (p85/p110) complex was purified on PY-beads from Sf9 cells infected with p85 and p110 recombinant baculovirus. [^{35}S]methionine-labeled p85 subunit ([^{35}S]p85) was generated using Promega's TNT quick coupled Transcription/Translation Kit according to the manufacturer's instructions. GST fusion proteins (30–50 mg) conjugated to glutathione sepharose beads were incubated overnight with recombinant PI3K complex or [^{35}S]p85 in RIPA buffer. The pellets were then washed three times with the same buffer. Affinity-precipitated PI3K complexes were detected by the PI3K activity assay described below. For detecting [^{35}S]p85 precipitated by GST fusion proteins, the pellets were eluted using 2× sample buffer and then subjected to SDS-PAGE and autoradiography.

Immunoprecipitation, Western Blotting, and PI3K Assays

Hippocampal slices (300 μm thickness) were prepared from adult Sprague-Dawley rats (150–200 g) and maintained in standard artificial cerebrospinal fluid aerated with 95% O_2/5% CO_2 at room tem-

perature as described elsewhere (Man et al., 2000b). Following a 1 hr recovery period, slices were subjected to various drug treatments for 5–10 min. Control slices and slices treated with either NMDA (50 μM), AMPA (50 μM), glycine (200 μM), or glycine + APV (50 μM) in the presence of the glycine receptor antagonist strychnine (10 μM) were then homogenized in RIPA buffer (50 mM Tris-HCl, 150 mM NaCl, 1% Triton X-100, 0.5% deoxycholate, 0.1% SDS, 1 mM orthovanadate). For some experiments where no drug treatment was involved, brain hippocampus (500 mg) was homogenized in buffer containing 50 mM Tris-Cl (pH 7.6), 150 mM NaCl, 1% Igepal CA-630, 0.5%–1% sodium deoxycholate, 2 mM EDTA, 1 mM sodium orthovanadate, 1 mM PMSF, and protease inhibitor cocktail (5 μl/100 mg tissue, Sigma). Tissue homogenates were centrifuged at 10,000 × *g* at 4°C for 20 min. Membrane pellets were further solubilized for 1 hr on ice with 1% Triton X-100 and centrifuged at 48,000 × *g* for 20 min. The supernatant containing about 500 μg of protein was then incubated with anti-p85 (2 μg, Upstate Biotechnology) or anti-GluR2 antibodies (2 μg, Chemicon International, Inc. or Upstate Biotechnology) in 500 μl RIPA buffer for 4 hr at 4°C. The antibody-protein complexes were then precipitated with protein A-Sepharose beads. For peptide interfering experiments, tissue lysates (500–700 μg) were incubated with one of the indicated GST fusion proteins (50 μg each) for 4 hr at 4°C before the primary antibody against the GluR2 subunit (2 μg, Upstate Biotechnology) was added, followed by the addition of 20 μl of protein A/G Sepharose (Sigma) for 12 hr. For immunoprecipitation under denaturing conditions, lysates were boiled for 5 min prior to incubation with the anti-p85 antibody. Proteins eluted from the beads were subjected to SDS-PAGE and immunoblotting for PI3K, GluR2, GluR1, and/or NR1 sequentially.

PI3K activity in the anti-GluR2 or anti-p85 immunoprecipitated protein complexes was assayed using the immunocomplex PI3K activity assay described previously (Wang et al., 1998). In brief, immunoprecipitates were washed sequentially on ice using washing buffers I (PBS containing 1% Nonidet P-40), II (0.5 M LiCl, 0.1 M Tris, pH 7.5), and III (10 mM Tris pH 7.5, 100 mM NaCl). The pellets were then mixed with phosphatidylinositol (PI) solution (50 ml of washing buffer III, 10 ml of 100 mM $MgCl_2$, 10 ml of PI suspension [Sigma]), and the reaction was started by adding 5 ml ^{32}P-γ-ATP. The reaction was stopped 10 min later with 10 ml HCl and 160 ml $CHCl_3$/MeOH mixture (1:1). The resulting phosphatidylinositol 3′-monophosphate (PI3-^{32}P) was separated from PI on a TLC plate and quantified using a Molecular Dynamics PhosphorImager System (Sunnyvale, CA).

Data Analysis

Values are expressed as Mean ± SE, and analyzed using a Student's t test for comparison between two groups and ANOVA for comparisons among multiple groups. Statistical significance is defined as $p < 0.05$.

Acknowledgments

This work was supported by research grants from the Heart and Stroke Foundation of Ontario/British Columbia and Yukon (T-4824, to Y.T.W.), the Canadian Institutes of Health Research (CIHR; to J.F.M. and Y.T.W.), the EJLB Foundation (Y.T.W.), and the Swiss National Science Foundation (3100-050506.97 to M.P.W.). Y.T.W. is an International Scholar of the Howard Hughes Medical Institute, an Investigator of the CIHR, a Senior Scholar of the Michael Smith Foundation for Health Research, and the holder of the Heart and Stroke Foundation of British Columbia and Yukon Chair in Stroke Research at the University of British Columbia and Vancouver Hospital and Health Sciences Centre. We thank G. Bulgarelli-Leva and B. Vukusic for excellent technical support and S. Van Iderstine for his excellent editorial assistance.

Received: May 1, 2002
Revised: February 28, 2003
Accepted: April 15, 2003
Published: May 21, 2003

References

Bayer, K.U., De Koninck, P., Leonard, A.S., Hell, J.W., and Schulman, H. (2001). Interaction with the NMDA receptor locks CaMKII in an active conformation. Nature *411*, 801–805.

Bear, M.F., and Malenka, R.C. (1994). Synaptic plasticity: LTP and LTD. Curr. Opin. Neurobiol. *4*, 389–399.

Beattie, E.C., Carroll, R.C., Yu, X., Morishita, W., Yasuda, H., von Zastrow, M., and Malenka, R.C. (2000). Regulation of AMPA receptor endocytosis by a signaling mechanism shared with LTD. Nat. Neurosci. *3*, 1291–1300.

Bliss, T.V.P., and Collingridge, G.L. (1993). A synaptic model of memory: Long-term potentiation in the hippocampus. Nature *361*, 31–39.

Carpenter, C.L., and Cantley, L.C. (1996). Phosphoinositide kinases. Curr. Opin. Cell Biol. *8*, 153–158.

Carroll, R.C., Lissin, D.V., von Zastrow, M., Nicoll, R.A., and Malenka, R.C. (1999). Rapid redistribution of glutamate receptors contributes to long-term depression in hippocampal cultures. Nat. Neurosci. *2*, 454–460.

Cheever, M.L., Sato, T.K., de Beer, T., Kutateladze, T.G., Emr, S.D., and Overduin, M. (2001). Phox domain interaction with PtdIns(3)P targets the Vam7 t-SNARE to vacuole membranes. Nat. Cell Biol. *3*, 613–618.

Daw, M.I., Bortolotto, Z.A., Saulle, E., Zaman, S., Collingridge, G.L., and Isaac, J.T. (2002). Phosphatidylinositol 3 kinase regulates synapse specificity of hippocampal long-term depression. Nat. Neurosci. *5*, 835–836.

De Camilli, P., Emr, S.D., McPherson, P.S., and Novick, P. (1996). Phosphoinositides as regulators in membrane traffic. Science *271*, 1533–1539.

Downward, J. (1997). Role of phosphoinositide-3-OH kinase in Ras signaling. Adv. Second Messenger Phosphoprotein Res. *31*, 1–10.

Hayashi, Y., Shi, S.H., Esteban, J.A., Piccini, A., Poncer, J.C., and Malinow, R. (2000). Driving AMPA receptors into synapses by LTP and CaMKII: requirement for GluR1 and PDZ domain interaction. Science *287*, 2262–2267.

Heller-Harrison, R.A., Morin, M., Guilherme, A., and Czech, M.P. (1996). Insulin-mediated targeting of phosphatidylinositol 3-kinase to GLUT4-containing vesicles. J. Biol. Chem. *271*, 10200–10204.

Hisatsune, C., Umemori, H., Mishina, M., and Yamamoto, T. (1999). Phosphorylation-dependent interaction of the N-methyl-D-aspartate receptor epsilon 2 subunit with phosphatidylinositol 3-kinase. Genes Cells *4*, 657–666.

James, D.E., and Piper, R.C. (1994). Insulin resistance, diabetes, and the insulin-regulated trafficking of GLUT-4. J. Cell Biol. *126*, 1123–1126.

Joyal, J.L., Burks, D.J., Pons, S., Matter, W.F., Vlahos, C.J., White, M.F., and Sacks, D.B. (1997). Calmodulin activates phosphatidylinositol 3-kinase. J. Biol. Chem. *272*, 28183–28186.

Kelly, A., and Lynch, M.A. (2000). Long-term potentiation in dentate gyrus of the rat is inhibited by the phosphoinositide 3-kinase inhibitor, wortmannin. Neuropharmacology *39*, 643–651.

Kim, J.H., and Huganir, R.L. (1999). Organization and regulation of proteins at synapses. Curr. Opin. Cell Biol. *11*, 248–254.

Kim, C.H., Chung, H.J., Lee, H.K., and Huganir, R.L. (2001). Interaction of the AMPA receptor subunit GluR2/3 with PDZ domains regulates hippocampal long-term depression. Proc. Natl. Acad. Sci. USA *98*, 11725–11730.

Kuruvilla, R., Ye, H., and Ginty, D.D. (2000). Spatially and functionally distinct roles of the PI3-K effector pathway during NGF signaling in sympathetic neurons. Neuron *27*, 499–512.

Liang, F., and Huganir, R.L. (2001). Coupling of agonist-induced AMPA receptor internalization with receptor recycling. J. Neurochem. *77*, 1626–1631.

Liao, D., Scannevin, R.H., and Huganir, R. (2001). Activation of silent synapses by rapid activity-dependent synaptic recruitment of AMPA receptors. J. Neurosci. *21*, 6008–6017.

Lin, J.W., Ju, W., Foster, K., Lee, S.H., Ahmadian, G., Wyszynski,

M., Wang, Y.T., and Sheng, M. (2000). Distinct molecular mechanisms and divergent endocytotic pathways of AMPA receptor internalization. Nat. Neurosci. *3*, 1282–1290.

Lin, C.H., Yeh, S.H., Lin, C.H., Lu, K.T., Leu, T.H., Chang, W.C., and Gean, P.W. (2001). A role for the PI-3 kinase signaling pathway in fear conditioning and synaptic plasticity in the amygdala. Neuron *31*, 841–851.

Lisman, J., Schulman, H., and Cline, H. (2002). The molecular basis of CaMKII function in synaptic and behavioural memory. Nat. Rev. Neurosci. *3*, 175–190.

Lu, W., Man, H., Ju, W., Trimble, W.S., MacDonald, J.F., and Wang, Y.T. (2001). Activation of synaptic NMDA receptors induces membrane insertion of new AMPA receptors and LTP in cultured hippocampal neurons. Neuron *29*, 243–254.

Luscher, C., Xia, H., Beattie, E.C., Carroll, R.C., von Zastrow, M., Malenka, R.C., and Nicoll, R.A. (1999). Role of AMPA receptor cycling in synaptic transmission and plasticity. Neuron *24*, 649–658.

Malenka, R.C., and Nicoll, R.A. (1999). Long-term potentiation–a decade of progress? Science *285*, 1870–1874.

Malinow, R., Mainen, Z.F., and Hayashi, Y. (2000). LTP mechanisms: from silence to four-lane traffic. Curr. Opin. Neurobiol. *10*, 352–357.

Man, H.Y., Ju, W., Ahmadian, G., and Wang, Y.T. (2000a). Intracellular trafficking of AMPA receptors in synaptic plasticity. Cell. Mol. Life Sci. *57*, 1526–1534.

Man, H.Y., Lin, J.W., Ju, W.H., Ahmadian, G., Liu, L., Becker, L.E., Sheng, M., and Wang, Y.T. (2000b). Regulation of AMPA receptor-mediated synaptic transmission by clathrin-dependent receptor internalization. Neuron *25*, 649–662.

Nishiyama, M., Hong, K., Mikoshiba, K., Poo, M.M., and Kato, K. (2000). Calcium stores regulate the polarity and input specificity of synaptic modification. Nature *408*, 584–588.

Passafaro, M., Piech, V., and Sheng, M. (2001). Subunit-specific temporal and spatial patterns of AMPA receptor exocytosis in hippocampal neurons. Nat. Neurosci. *4*, 917–926.

Pessin, J.E., Thurmond, D.C., Elmendorf, J.S., Coker, K.J., and Okada, S. (1999). Molecular basis of insulin-stimulated GLUT4 vesicle trafficking. Location! Location! Location! J. Biol. Chem. *274*, 2593–2596.

Rapoport, I., Miyazaki, M., Boll, W., Duckworth, B., Cantley, L.C., Shoelson, S., and Kirchhausen, T. (1997). Regulatory interactions in the recognition of endocytic sorting signals by AP-2 complexes. EMBO J. *16*, 2240–2250.

Rodriguez-Viciana, P., Warne, P.H., Vanhaesebroeck, B., Waterfield, M.D., and Downward, J. (1996). Activation of phosphoinositide 3-kinase by interaction with Ras and by point mutation. EMBO J. *15*, 2442–2451.

Sanna, P.P., Cammalleri, M., Berton, F., Simpson, C., Lutjens, R., Bloom, F.E., and Francesconi, W. (2002). Phosphatidylinositol 3-kinase is required for the expression but not for the induction or the maintenance of long-term potentiation in the hippocampal CA1 region. J. Neurosci. *22*, 3359–3365.

Shen, K., and Meyer, T. (1999). Dynamic control of CaMKII translocation and localization in hippocampal neurons by NMDA receptor stimulation. Science *284*, 162–166.

Sheng, M., and Lee, S.H. (2001). AMPA receptor trafficking and the control of synaptic transmission. Cell *105*, 825–828.

Sheng, M., and Sala, C. (2001). Pdz domains and the organization of supramolecular complexes. Annu. Rev. Neurosci. *24*, 1–29.

Shi, S.H., Hayashi, Y., Petralia, R.S., Zaman, S.H., Wenthold, R.J., Svoboda, K., and Malinow, R. (1999). Rapid spine delivery and redistribution of AMPA receptors after synaptic NMDA receptor activation. Science *284*, 1811–1816.

Shpetner, H., Joly, M., Hartley, D., and Corvera, S. (1996). Potential sites of PI-3 kinase function in the endocytic pathway revealed by the PI-3 kinase inhibitor, wortmannin. J. Cell Biol. *132*, 595–605.

Soderling, T.R., and Derkach, V.A. (2000). Postsynaptic protein phosphorylation and LTP. Trends Neurosci. *23*, 75–80.

Stenmark, H., and Aasland, R. (1999). FYVE-finger proteins–effectors of an inositol lipid. J. Cell Sci. *112*, 4175–4183.

Vanhaesebroeck, B., Leevers, S.J., Panayotou, G., and Waterfield, M.D. (1997). Phosphoinositide 3-kinases: a conserved family of signal transducers. Trends Biochem. Sci. *22*, 267–272.

Wang, Y.T., and Linden, D.J. (2000). Expression of cerebellar long-term depression requires postsynaptic clathrin-mediated endocytosis. Neuron *25*, 635–647.

Wang, Q., Bilan, P.J., Tsakiridis, T., Hinek, A., and Klip, A. (1998). Actin filaments participate in the relocalization of phosphatidylinositol3-kinase to glucose transporter-containing compartments and in the stimulation of glucose uptake in 3T3–L1 adipocytes. Biochem. J. *331*, 917–928.

Wenthold, R.J., Petralia, R.S., Blahos, J., II, and Niedzielski, A.S. (1996). Evidence for multiple AMPA receptor complexes in hippocampal CA1/CA2 neurons. J. Neurosci. *16*, 1982–1989.

Wymann, M.P., and Pirola, L. (1998). Structure and function of phosphoinositide 3-kinases. Biochim. Biophys. Acta *1436*, 127–150.

Wymann, M.P., Bulgarelli-Leva, G., Zvelebil, M.J., Pirola, L., Vanhaesebroeck, B., Waterfield, M.D., and Panayotou, G. (1996). Wortmannin inactivates phosphoinositide 3-kinase by covalent modification of Lys-802, a residue involved in the phosphate transfer reaction. Mol. Cell. Biol. *16*, 1722–1733.

Yang, J., Clarke, J.F., Ester, C.J., Young, P.W., Kasuga, M., and Holman, G.D. (1996). Phosphatidylinositol 3-kinase acts at an intracellular membrane site to enhance GLUT4 exocytosis in 3T3–L1 cells. Biochem. J. *313*, 125–131.

Zamanillo, D., Sprengel, R., Hvalby, O., Jensen, V., Burnashev, N., Rozov, A., Kaiser, K.M., Koster, H.J., Borchardt, T., Worley, P., et al. (1999). Importance of AMPA receptors for hippocampal synaptic plasticity but not for spatial learning. Science *284*, 1805–1811.

Zhu, J., Qin, Y., Zhao, M., Van Aelst, L., and Malinow, R. (2002). Ras and Rap control AMPA receptor trafficking during synaptic plasticity. Cell *110*, 443–455.

Zhuo, M., and Hawkins, R.D. (1995). Long-term depression: a learning-related type of synaptic plasticity in the mammalian central nervous system. Rev. Neurosci. *6*, 259–277.

Zorumski, C.F., and Thio, L.L. (1992). Properties of vertebrate glutamate receptors: Calcium mobilization and desensitization. Prog. Neurobiol. *39*, 295–336.